Estimation of the load-bearing capacity of tubular cantilever beams containing through-thickness circumferential U-notches

S. Cicero[1,*], M. Sánchez[1], B. Arroyo[1], J.D.Fuentes[1], J.A.Álvarez[1]

Laboratory of Materials Science and Engineering, University of Cantabria, E.T.S. de Ingenieros de Caminos, Canales y Puertos, Av/Los Castros 44, Santander 39005, Spain

* corresponding author: ciceros@unican.es

Abstract

This paper provides a methodology for the structural integrity assessment of tubular beams containing U-notches, and particularises the analysis to the case of cantilever beams containing through thickness U-notches. The methodology is based on the combined use of Failure Assessment Diagrams and the Theory of Critical Distances, with the BS7910 as the reference fracture assessment document. The results, obtained in Al6060 and PVC (Polyvinyl chloride) tubular cantilever beams, demonstrates that the proposed approach provides accurate predictions of failure loads.

Keywords: load-bearing capacity; fracture; tube; through-thickness notch; U-notch; cantilever beam

Nomenclature

a	one half of the defect length
E	material elastic modulus
f_w	geometric parameter defined in BS7910 Annex M
J	applied J-integral
J_e	elastic component of J
K_{eff}	effective stress intensity factor used in mixed-mode analyses (defined from K_I, K_{II} and K_{III})
K_{Jc}	elastic-plastic fracture resistance derived from the J-integral at the point of onset of fracture
K_{mat}	material fracture resistance measured by the stress intensity factor
K^N_{mat}	apparent fracture toughness
K_r	fracture ratio of applied K_I to fracture resistance
K_I	stress intensity factor (mode I loading)
K_{II}	stress intensity factor (mode II loading)
K_{III}	stress intensity factor (mode III loading)
K_{IC}	material fracture toughness in plane strain linear-elastic conditions
K_{Inotch}	notch stress intensity factor
L	material critical distance
L_r	ratio of applied load to limit load (or reference stress to yield stress)
L_r^{max}	maximum value of L_r in a FAD

P	applied load
P_L	limit load
$P_{m,b}$	primary membrane stress due to global bending moment
r	distance from the notch tip
r_i	inner radius
r_m	mean radius
r_0	outer radius
M,	geometric parameter defined in BS7910 Annex M
M_1	geometric parameter defined in BS7910 Annex M
M_2	geometric parameter defined in BS7910 Annex M
β	geometric parameter defined in BS7910 Annex M εref
ρ	notch radius
σ	applied stress
σ_{coh}	cohesive stress ahead of the crack tip
σ_{ref}	reference stress
σ_u	ultimate tensile strength
σ_y	yield stress
σ_0	material strength parameter (the inherent strength)
ASED	Averaged Strain Energy Criterion
CT	Compact Tension (specimen)
FAD	Failure Assessment Diagram
FAL	Failure Assessment Line
LBC	Load Bearing Capacity
LM	Line Method
PM	Point Method
SENB	Single Edge Notched Bending (specimen)
TCD	Theory of Critical Distances

1. Introduction

Tubular sections are widely used in many engineering applications, from pipes to structural profiles used in bridges, offshore structures or buildings, among others. In most of them, their primary function (together with fluid conveyance in the case of pipes) is structural (i.e., they must conveniently and

safely sustain different types of loads). Thus, the estimation of the load-bearing capacity of this kind of structural sections is a significant issue in engineering practice. This estimation is particularly sensitive when the tubular sections contain defects such as cracks or notches, given that these defects may significantly reduce the corresponding load-bearing capacity.

When cracks are present, fracture mechanics (e.g., [1,2]) and well-known structural integrity standards/procedures (e.g., [3-6]) allow fracture-plastic collapse analyses to be performed by using well-known comprehensive validated methodologies. Fracture mechanics concepts, as well as analytical solutions for stress intensity factors and plastic collapse loads (or reference stresses) are available for a wide range of practical situations. However, when dealing with notches, the situation is not so well-defined. One could always assess notches as if they were cracks, but literature demonstrates (e.g., [7-10]) that this practice is generally over-conservative. The main source of this conservatism is that materials containing notches develop a fracture resistance that may be much higher than the material fracture toughness measured in cracked conditions. In this work, the fracture resistance developed in notched conditions will be referred to as the apparent fracture toughness, with the term fracture toughness being only used for the fracture resistance obtained in cracked conditions.

With the aim of providing accurate methodologies for the assessment (e.g., load-bearing capacity estimation) of structural components containing notches, some methodologies based on the use of Failure Assessment Diagrams (FADs) have been provided in the last years. Some of them are those provided by Smith [11,12], Matvienko [13,14], Cicero et al. [15,16], and Horn and Sherry [17,18].

Smith [11,12] states that there is a geometry dependence of the Failure Assessment Line (FAL), and quantifies this dependence for the case of a blunt flaw [11] and a sharp groove [12], with the fracture ratio (K_r) being defined in terms of an effective stress intensity factor, as if the flaw were a crack. Matvienko [13,14] generates the FAD from the Dugdale-Barenblatt cohesive zone model [19,20] and the Novozhilov average stress criterion [21], leading to a Failure Assessment Line that depends on the type of loading and the elastic stress concentration factor. The approach represents the normalised stress intensity factor (K_{Inotch}/K_{IC}) vs. the normalised applied stress (σ/σ_{coh}), where K_{Inotch} is the stress intensity factor at the notch tip, K_{IC} is the material fracture toughness, σ is the applied remote stress, and σ_{coh} is the cohesive stress (see [11] for details). Cicero et al [9,15,16], propose a methodology (explained in detail in Section 3) in which the only difference between cracks and notches when using FADs is the material fracture resistance considered in the definition of the fracture ratio K_r: the fracture toughness, K_{mat}, when analysing cracks, and the apparent fracture toughness, K^N_{mat}, when dealing with notches. The apparent fracture toughness is derived by using the Theory of Critical Distances [7], and the rest of inputs required for the assessment are exactly the same as those used for crack-like defects in structural integrity and facture assessment procedures (e.g., [3,6]), including the stress intensity factor, the plastic collapse load and the FAL itself. Finally, Horn and Sherry [17,18] defined an engineering assessment methodology for ferritic steel structures containing non-sharp defects (i.e., notches). This methodology can be applied with different levels of accuracy, depending on how the parameters describing the sensitivity of the material fracture toughness to the notch effect are measured: testing notched specimens of the same thickness as the structure, or (for cleavage fracture) obtained using look-up tables generated using the Weibull stress toughness scaling model.

These methods have been generally validated by using experimental results obtained in fracture specimens, mainly compact tension (CT) and single edge notched bending (SENB) specimens, with (to the knowledge of the authors) very limited data on structural components.

Finally, it is important to notice that the assessment of notches can be performed by using other approaches, different to the TCD, with extensive validation in literature by using fracture specimens but, again, limited results on structural applications. Some examples, based on the Averaged Strain Energy Density (ASED) criterion, may be found in [22-26].

In this context, this paper particularises the methodology proposed by Cicero et al. to the analysis of tubular cantilever beams containing U-notches, and describes an experimental programme that is used to validate this approach. With this aim, Section 2 provides the theoretical framework of the work, including a description of both the FAD methodology and the Theory of Critical Distances. Section 3 presents the methodology proposed for the assessment of U-notched tubular cantilever beams, Section 4 includes a description of the experimental program and gathers the experimental results, Section 5 gathers the load-bearing capacity predictions provided by the proposed methodology, and discusses the results, and Section 6 presents the main conclusions.

2. Theoretical framework: Failure Assessment Diagrams and the Theory of Critical Distances

Failure Assessment Diagrams (FADs) are currently the main engineering tool for the assessment of fracture-plastic collapse processes in cracked components. They were first proposed by Dowling and Townley [27] and Harrison et al. [28], who derived them from the modified version of the Burdekin and Stone [29] strip yield model [19,20]. Nowadays, they are included in the most significant structural integrity assessment procedures and standards (e.g., [3-6]).

When performing the assessment of a given cracked structural component, the FAD methodology presents a simultaneous assessment of both fracture and plastic collapse processes by using two normalised parameters, K_r (fracture ratio) and L_r (plastic collapse ratio). For mode I loading conditions:

$$K_r = \frac{K_I}{K_{mat}} \quad (1)$$

$$L_r = \frac{P}{P_L} \quad (2)$$

P being the applied load, P_L the limit load, K_I the stress intensity factor, and K_{mat} the material fracture resistance measured by the stress intensity factor (e.g., K_{IC}, K_{Jc}, etc). In certain documents, such as the BS7910 [4], L_r is expressed following equation (3), which is equivalent to equation (2) [4]:

$$L_r = \frac{\sigma_{ref}}{\sigma_Y} \quad (3)$$

σ_{ref} being the reference stress, which is obtained by multiplying equation (2) by the yield stress, and σ_Y being the material yield stress.

These definitions imply that K_r evaluates the component against fracture, whereas L_r evaluates the structural component situation against plastic collapse. The component being analysed is represented by a point of coordinates (K_r, L_r) that has to be compared with the component limiting conditions (those causing the final failure). Such conditions are defined by the Failure Assessment Line (FAL): if the assessment point is located between the FAL and the coordinate axes, the component is considered to be under safe conditions; if the assessment point is located above the FAL, the component is considered to be under unsafe conditions; finally, the critical situation (failure) is that in which the assessment point lies exactly on the FAL [3-6]. Figure 1 shows an example with the three different possible situations when performing fracture initiation analyses.

The FAL follows expressions that are functions of L_r:

$$K_r = f(L_r) \tag{4}$$

These $f(L_r)$ functions are essentially plasticity corrections to the linear-elastic fracture assessment (K_r=1). Their rigorous analytical solution is:

$$f(L_r) = \sqrt{\frac{J_e}{J}} \tag{5}$$

J being the applied J-integral and J_e its corresponding elastic component [1,2].

This analysis is additionally limited by the cut-off, which corresponds to the load level causing the plastic collapse of the analysed component. This cut-off is defined by the maximum value of L_r (L_r^{max} in Figure 1), which depends on the material flow stress, generally defined as the average value of the material yield stress and ultimate tensile strength.

The definition of $f(L_r)$ following equation (5) is not straightforward and would generally require finite element analysis. Although structural integrity assessment procedures [3-6] include this possibility, in practical terms, they also provide approximate solutions to equation (5) that may be easily defined through the tensile properties of the material. These solutions are usually provided hierarchically, defining different levels on which the more defined the material stress-strain curve, the more approximate are such solutions to equation (5). For example, BS7910 [4] defines Option 1, which requires both the yield or proof strength and the ultimate tensile strength. For materials exhibiting continuous yielding behaviour, Option 1 is defined by equations (6) to (11):

$$K_r = f(L_r) = \left[1 + \frac{1}{2}(L_r)^2\right]^{-1/2} \cdot \left[0.3 + 0.7 \cdot e^{-\mu \cdot (L_r)^6}\right] \qquad L_r \leq 1 \tag{6}$$

$$K_r = f(L_r) = f(1) \cdot L_r^{\frac{N-1}{2N}} \qquad 1 < L_r \leq L_r^{max} \tag{7}$$

$$K_r = f(L_r) = 0 \qquad L_r = L_r^{max} \tag{8}$$

$$\mu = min\left[0.001 \cdot \frac{E}{\sigma_Y}; 0.6\right] \tag{9}$$

$$N = 0.3 \cdot \left(1 - \frac{\sigma_Y}{\sigma_u}\right) \tag{10}$$

$$L_r^{max} = \frac{\sigma_Y + \sigma_u}{2 \cdot \sigma_Y} \tag{11}$$

Option 1 FAD is the most simple analysis option of BS7910 and, in fact, it is the most commonly used in engineering assessments.

On the other hand, BS 7910 Option 2 requires the full stress-strain curve and is defined by equations (11) to (13):

$$K_r = f(L_r) = \left(\frac{E\varepsilon_{ref}}{L_r\sigma_y} + \frac{L_r^3\sigma_y}{2E\varepsilon_{ref}}\right)^{-1/2} \qquad L_r < L_r^{max} \tag{12}$$

where ε_{ref} is the true strain at the true stress $\sigma_{ref} = L_r \cdot \sigma_y$

$$f(L_r) = 0 \qquad L_r > L_r^{max} \qquad (13)$$

L_r^{max} also follows equation (11).

Finally, Option 3 in BS7910 corresponds to the exact solution of the FAL, provided by equations (4) and (5), and with the cut-off following the same definition of options 1 and 2.

Although the FAD methodology is proposed in structural integrity procedures (e.g. [3-6]) for metallic materials, Fuentes and Cicero [30] demonstrated that this methodology may also be applied to polymeric materials such as PMMA and PA6, among other non-metals. Therefore, here it is applied not only to Al6060, but also to PVC tubular beams.

From an engineering and practical perspective, the fracture analysis performed by using the FAD approach is based on a linear-elastic parameter (K_I), irrespective of the plasticity level existing on the crack tip. Additionally, structural integrity assessment procedures provide K_I and P_L (or σ_{ref}) solutions for a wide variety of components (plates, pipes, spheres…) and crack geometries (surface cracks, through-thickness crack, corner crack…), something that simplifies the completion of structural integrity assessments.

Concerning the Theory of Critical Distances (TCD), it is actually a set of methodologies, all of which use a material length parameter (L, the critical distance) when performing fracture analyses. It may also be applied to subcritical processes, such as fatigue [7] and environmentally assisted cracking [31]. The origin of the TCD is found in the works of Neuber [32] and Peterson [33], but it has been in the last two decades that this theory has been thoroughly developed.

The critical distance in fracture analyses follows equation (14):

$$L = \frac{1}{\pi}\left(\frac{K_{mat}}{\sigma_0}\right)^2 \qquad (14)$$

where K_{mat} is the material fracture resistance in cracked conditions and σ_0 is a material strength parameter usually referred to as the inherent strength. This parameter is usually larger than the ultimate tensile strength (σ_u), requiring the corresponding calibration. Only in those materials with linear-elastic behaviour at both the micro and the macro scales (e.g., fracture of ceramics) does σ_0 coincide with σ_u. In such cases, there is no need for any calibration for the application of the TCD, as long as L is directly obtained from equation (14), K_{mat} and σ_u.

Among the different methodologies included within the TCD, the Point Method (PM) and the Line Method (LM) are the most widely known. Both are based on the stress field at the defect tip and their corresponding predictions are very similar [7].

The PM is the simplest methodology. It states that fracture occurs when the stress at a distance of L/2 from the defect tip reaches the inherent strength (σ_0):

$$\sigma\left(\frac{L}{2}\right) = \sigma_0 \qquad (15)$$

Alternatively, the LM states that fracture takes place when the average stress along a distance equal to 2L (from the defect tip) reaches the inherent strength σ_0:

$$\frac{1}{2L}\int_0^{2L} \sigma(r)\, dr = \sigma_0 \qquad (16)$$

The TCD (and its different methodologies, including the PM and the LM) allows the fracture assessment of components containing notches to be performed. However, for those materials in which σ_0 does not coincide with σ_u (e.g., most polymers, metals, etc), the former parameter requires calibration. This may be performed by undertaking an experimental programme on notched specimens with different notch radii, by finite elements simulation of specimens with different notch radii, or by a combination of experimental programme and finite elements modelling.

Both the PM and the LM may generate predictions of the apparent fracture toughness (K^N_{mat}) developed by components containing U-shaped notches. When using PM, it is necessary to consider the stress distribution on the notch tip provided by Creager and Paris [34], which is equal to that ahead of the crack tip but displaced a distance equal to ρ/2 along the x-axis:

$$\sigma(r) = \frac{K_I}{\sqrt{\pi}} \frac{2\cdot(r+\rho)}{(2r+\rho)^{3/2}} \tag{17}$$

where K_I is the mode I stress intensity factor corresponding to a crack with the same dimensions of the notch, ρ is the notch radius and r is the distance existing from the notch tip to the point being assessed.

Now, considering both the condition defining the PM (equation (15)) and the definition of the critical distance L (equation (14)), and assuming that fracture occurs when K_I is equal to K^N_{mat}, equation (18) can be obtained [7]:

$$K^N_{mat} = K_{mat} \frac{\left(1+\frac{\rho}{L}\right)^{3/2}}{\left(1+\frac{2\rho}{L}\right)} \tag{18}$$

Likewise, the application of the LM leads to equation (19) [7]:

$$K^N_{mat} = K_{mat} \sqrt{1+\frac{\rho}{4L}} \tag{19}$$

These two predictions provide very similar results. Additional details on the TCD, its different approaches for the analysis of notch effect, and the resulting predictions, can be found in the literature (e.g., [7]).

3. Proposed methodology

This work proposes the analysis of tubular cantilever beams containing through-thickness U-notches by applying the general approach first presented in [15], and additionally validated in [9,16]. This validation was limited to ordinary fracture testing specimens (C(T) and SENB), so its application to real components remains as an engineering issue (this circumstance being also applicable to other methodologies, such as those briefly described above [11-14,17,18,22-26]).

The general approach proposes converting a notched material with K_{mat} as the fracture resistance into an equivalent situation with a cracked material having a higher fracture resistance, equal to K^N_{mat}. Under this assumption, the definition of the K_r parameter would follow equation (20) if the LM formulation is considered:

$$K_r = \frac{K_I}{K^N_{mat}} = \frac{K_I}{K_{mat}\sqrt{1+\frac{\rho}{4L}}} \tag{20}$$

Equation (20) substitutes equation (1) when the defects being analysed are U-shaped notches. The FAD analysis also needs to define the Lr parameter, which depends on the limit load (equation (2)).

On the other hand, plastic collapse occurs through the yielding of the remnant section, so that in a perfectly plastic material, it can be defined by the material yield stress and the defect dimensions, with no influence of the radius existing on the defect tip. The relatively low influence of the notch radius on the limit load is demonstrated in [35], and assuming the limit load solutions for cracks when analysing notches with the same geometry (but for the notch radius) is just a slightly conservative practice [35-37].

The last aspect requiring definition to complete the FAD analysis of notches is the FAL to be used. Horn and Sherry demonstrated a weak dependence of the R6 Option 3 failure assessment lines (Option 3 in BS7910 as well) on the notch radius [17,18]. Thus, when analysing notch-type defects, the use of the FALs proposed for crack assessments in BS7910 [4] and other structural integrity assessment procedures (e.g., [3,5,6]) does not generate significant inaccuracies.

Consequently, from a practical point of view, the proposed general approach for the assessment of notches only requires the K_r parameter to be adjusted, using the same L_r (P_L or σ_{ref} solutions) and FAL equations defined for the assessment of crack-like defects. Beyond the validation of the methodology presented by the authors in previous works (e.g., [9,15,16]), Horn et al. [36,37] have also demonstrated and commented about the small errors that may be expected when considering the assumptions adopted by the approach proposed here.

The particularisation of the general approach to the assessment of tubular cantilever beams containing through-thickness circumferential U-notches is performed by using the K_I and σ_{ref} solutions provided by the BS7910 [4] for through-thickness cracks. Assuming that tubes are thin-walled and only subjected to bending loads, the stress state is simplified by a simple primary membrane stress due to global bending moment ($P_{m,b}$). The whole set of formulae is the following (when considering Option 1 FAL):

- FAL: equations (6) to (11)
- K_r: equation (20), with

  K^N_{mat}: equation (19), and

  $$K_I = \left\{ f_w \cdot \left[(M_1 + M_2) \cdot \beta \cdot P_{m,b} \right] \right\} \cdot \sqrt{\pi \cdot a} \qquad (21)$$

  f_w, M, M_1, M_2 and β are geometric parameters provided by formulae or tables in BS7910 Annex M (section M.7.3.1 [4]). Equation (21) assumes that there are no secondary stresses. In case there were secondary stresses in the component being analysed (or any other source of primary stresses), the process would be analogous with the stress intensity factor expression (K_I) provided by BS7910 for such circumstances. Equation (21) also assumes that there is no through-wall bending.
- L_r: equation (3), with:

  $$\sigma_{ref} = \frac{\pi \cdot P_{m,b} \cdot \left(r_o^4 - r_i^4\right)}{\left(\pi - \frac{a}{r_i} - 2 \cdot \frac{sin^2\left(\frac{a}{r_i}\right)}{\pi - \frac{a}{r_i}} - \frac{sin\left(\frac{2a}{r_i}\right)}{2}\right)\left(4 r_0 r_m^2 B\right)} \qquad (22)$$

equation (22) is a simplification of equation P.22 in BS7910, which leads to equation (22) when there are no axial forces and no internal pressure (membrane stresses are caused by global bending only). Thus, the only source of membrane stresses are those caused by the global bending moment being applied. r_0 is the outer radius, r_i is the inner radius, r_m is the mean radius, a is one half of the defect length (see Figure 2), and B the thickness of the tubular section.

For the purposes of this paper, once the geometries of both the defect (ρ,a) and the tubular section (e.g., r_i, r_0) are known, together with the material properties (σ_y,σ_u,K_{mat}, L), the corresponding critical load may be easily determined by (iteratively) providing values until the assessment point lies on the FAL. Figure 3 represents the methodology in a flowchart.

The methodology can be easily applied to other common practical situations. Some examples could be the following:

- For any other notch geometry (e.g., internal surface notch oriented circumferentially, fully circumferential external surface notch, etc), the analysis would just require the use of the corresponding K_I and σ_{ref} solutions.
- For mixed-mode loading conditions, BS7910 Annex A [4] should be followed. This Annex proposes the use of an effective stress intensity factor (K_{eff}), instead of K_I, derived from the applied K_I, K_{II} and K_{III}.
- For thicker tubes, on which the through-thickness effects of the stress field may play a key role, leading to fully plane strain conditions, this methodology would require considering appropriate K_I and σ_{ref} solutions, and defining K_{mat} from fracture specimens also fulfilling plane strain conditions.
- For low constraint conditions associated to shallow notches and tensile loads, a constraint correction factor may be applied to K_{mat}, as defined in BS7910 Annex N [3,4,38].

4. Experimental programme and (experimental) results

In order to validate the above described methodology on structural components, a total of six aluminium and PVC tubular cantilever beams were tested. This allowed the accuracy of the methodology to be verified in well-known materials, covering a metal and a polymer. Aluminium alloys are widely used in engineering. Specifically, medium strength 6060 alloys are mostly used in civil engineering, automotive industry and architecture, since it is easy to extrude complex sections and thin-wall components at a moderate cost, having also good weldability and corrosion resistance. Polyvinylchloride (PVC) is the third most used thermoplastic worldwide: among its applications in the field of engineering, one of the most common is the manufacture of water and gas pipes. It can be found, mainly, in two forms: plasticised (or flexible) PVC and non-plasticised (or rigid PVC).

Three 1.8 m long Al6060-T66 alloy tubular cantilever beams were tested. Two of them had an outer diameter of Φ312 mm and 6 mm of thickness, while the other was Φ260 mm and 5 mm thick. Its chemical composition [39] is presented in Table 1.

In the case of PCV, three non-plasticised (rigid) 1.8 m long tubular cantilever beams were tested. Two of them had an outer diameter of Φ200 mm and 3.7 mm of thickness, while the other one was Φ315 mm and 6.8 mm thick. Their manufacture was performed according to the standard UNE-EN ISO 1401 [40].

A first step, which was not only necessary for the proper characterisation of the materials, but also to carry out the subsequent structural integrity assessment of the tubular cantilever beams, was to determine the corresponding mechanical properties. In this sense, tensile and fracture tests were carried out. For this purpose, one additional tube of each material (Φ260 mm, 5 mm thick in the case of aluminium; Φ315 mm, 6.8 mm thick in the case of PVC) was employed to obtain tensile and fracture samples through machining techniques. Thus, the total amount of tubes used in the program was eight, four per material (three used in the structural validation tests and one used in the material characterization process).

Tensile tests were performed according to ASTM E8M [41] standard procedure in the case of aluminum, and ASTM D638 [42] in the case of PVC. Six tensile specimens, 3 from each material, were obtained with their length being oriented along the longitudinal axis of the tubes, and then perpendicular to the defect propagation at failure. Figure 4 shows the dimensions of the specimens, which were the same for both materials except for the thickness (coincident with the total thickness of the corresponding tube): Al6060-T66 specimens were 5 mm thick, while the thickness of PVC specimens was 6.8 mm.

The tensile specimens were tested at a continuous rate of 5 mm/min for both materials. The applied load, as well as the elongation (measured by an extensometer with 12.5 mm gauge length) were continuously recorded. The tensile properties of the materials are presented in Table 2.

Additionally, the fracture behaviour of the materials was characterised by testing Single Edge Bend SE(B) specimens, according to ASTM E1820 [43] for Al6060-T66 and ASTM D5045 [44] for PVC. A total of 18 SE(B) specimens, 9 from each material, were prepared in LC orientation, in accordance with the defect propagation in the cantilever beams, with the tensile stresses acting in the longitudinal direction of the tubular section, and the defects propagating along the circumferential direction. The specimens were obtained from the same tubes as the tensile specimens (Φ260 mm and 5 mm thick for Al6060-T66 and Φ315 mm and 6.8 mm thick for PVC). Given that the specimens needed to be prismatic, their final thickness was slightly lower than the tube wall thickness (4.9 mm for Al6060-T66 and 6.7 mm for PVC). The geometry of the fracture specimens is shown in Figure 5, where ρ indicates the notch radii.

Here, it should be noted that, considering the thickness of the different tubes and fracture specimens, the two materials are always operating beyond the plane stress onset, which is given by [7]:

$$K_{Plan\ Stress} = \sigma_Y (\pi B)^{1/2} \quad (23)$$

In other words, the values of fracture resistance obtained in the two materials are well beyond the values provided by equation (23). Therefore, specimens and beams are operating under equivalent fracture conditions (plane stress).

The fracture specimens presented three possible notch radii at the defect tip: ρ=0 mm (crack-like defects), ρ=1 mm and ρ=2 mm [7-10]. The defects with finite radii (ρ=1mm and ρ=2mm) were machined, whereas crack-like defects were obtained by performing fatigue pre-cracking according to ASTM E1820 [43], in the case of Al6060-T66, or by sawing a razor blade (as described in ASTM D5045 [44]) in the case of PVC.

With all this, three tests were carried out for each combination of notch radius and material, the testing rate being 10 mm/min in all cases. The results of the fracture tests are gathered in Table 3, with some load-displacement curves being shown in Figure 6. K^N_{mat} refers to the apparent fracture toughness, which is the material fracture resistance in notched conditions (for cracked specimens it coincides with the material fracture toughness).

The results obtained with the different notch radii allow the corresponding material critical distance (L) to be estimated. Figure 7 shows the experimental results together with the Line Method (LM) fitting by using the least squares methodology, L being the fitting parameter.

After the characterisation tests, and with the aim of performing the structural integrity assessments of the tubular cantilever beams containing U-notches, structural tests were prepared for the remaining six tubes. Through-thickness circumferential U-notches (Figure 2) were machined in the 1.8 m long tubular cantilever beams at a distance of approximately 350mm from one of the extremes. Then, a section of the tubes of 330 mm length was embedded in reinforced concrete, forming a solid block covering the beam up to a section located 20 mm away from the notch (this distance is here referred to as d). As a result, six encastred cantilever beams with l=1470mm were obtained, following the scheme shown in Figure 8. The geometric parameters of the different resulting beams and U-notches are gathered in Table 4, whereas Figure 9 shows an image of the experimental setup.

Once the tubular beams were prepared, they were placed on a testing bench, with the solid concrete block fixed with screws to avoid any displacement or rotation. To measure the deflection at the free edge, where the corresponding single vertical load was applied, a laser comparator was used. The testing rate was 10 mm/min and the results obtained (in terms of Load-Bearing Capacity, LBC_{exp}) are shown in the Table 4. Figure 10 shows the load-displacement (vertical displacement at free edge) curves.

5. Load-bearing capacity predictions

Once the experimental values of the Load-bearing capacity (e.g., critical loads) have been obtained, this section provides the corresponding estimations obtained using the model explained above. The FAD methodology has been applied to both Al6060-T66 and PVC tubular beams, considering the notch correction described in section 3.

The results are shown in Table 4 (LBC_{est}), with Figure 11 showing the corresponding FAD analyses. It can be observed how the assessment points have a clear vertical displacement (towards lower values of K_r) when the notch correction is applied. As a consequence, for the resulting failure loads (those leading to assessment points lying on the FAL), the corresponding assessments performed without notch correction provide assessment points in the unsafe area (i.e., if no notch correction is applied, the estimated failure loads are necessarily lower).

Figure 12 compares the resulting estimations with the experimental results, revealing that the load-bearing capacity estimations represent accurate safe predictions of the experimental critical loads. The average deviation from the experimental results is 9% for the Al6060-T66 beams, and 16% for the PVC beams, something that it is within the typical scatter range in fracture processes and whichis typically accepted in fracture research (e.g., [7-10]). These deviations increase up to 15% and 25%, respectively, in case no notch corrections are applied. This difference, which is noticeable in any case, is mitigated by the fact that failures took place for high values of L_r, and thus, for situations where the notch effect is less severe. It is important to notice that more brittle failures (lower L_r values at failure) would provide larger differences between the results obtained with and without notch correction.

6. Conclusions

This paper provides and validates a methodology for the structural integrity assessment of tubular beams containing U-notches. The methodology is based on the combined use of Failure Assessment Diagrams and the Theory of Critical Distances, with the BS7910 as the reference fracture assessment document and the calibration of the corresponding values of the critical distance being done by completing fracture tests on SENB specimens containing different notch radii. The validation is

performed on Al6060-T66 and PVC cantilever beams containing through-thickness U-notches with different lengths and radii, and the results demonstrate that the proposed approach provides accurate safe predictions of failure loads, generating significantly more precise results than those obtained when assuming that notches behave as cracks (and notch corrections are not applied).

Acknowledgements

The authors of this work would like to express their gratitude to the Spanish Ministry of Science and Innovation for the financial support of the projects MAT2014-58443-P and PGC2018-095400-B-I00 (MCI/AEI/FEDER, UE), on the results of which this paper is based.

References

[1] Anderson TL. Fracture Mechanics: Fundamentals and Applications. 4th ed. Boca Raton: CRC Press - Taylor and Francis Group; 2005.

[2] Broek D. Elementary engineering fracture mechanics. 4th ed. Dordrecht, The Netherlands: Martinus Nijhoff; 2012.

[3] Kocak M, Webster S, Janosch JJ, Ainsworth RA, Koers R. FITNET Fitness-for-Service (FFS) Procedure vol. 1. Hamburg: GKSS; 2008.

[4] BS7910, Guide to methods for assessing the acceptability of flaws in metallic structures. London: British Standards Institution; 2019.

[5] R6: assessment of the integrity of structures containing defects. Rev. 4. Gloucester, UK: EDF Energy; 2015.

[6] API 579-1/ASME FFS-1 Fitness-For-Service. Washington DC: API Publishing Services; 2016.

[7] Taylor D. The theory of critical distances: a new perspective in fracture mechanics. London, UK: Elsevier; 2007.

[8] Cicero S, Madrazo V, García T, Cuervo J, Ruiz E. On the notch effect in load bearing capacity, apparent fracture toughness and fracture mechanisms of polymer PMMA, aluminium alloy Al7075-T651 and structural steels S275JR and S355J2. Eng Fail Anal 2013;29:108–21.

[9] Cicero S, Madrazo V, García T. On the assessment of U-shaped notches using Failure Assessment Diagrams and the Line Method: experimental overview and validation. Theor Appl Fract Mec 2015;80:235–41.

[10] Berto F, Lazzarin P. Recent developments in brittle and quasi-brittle failure assessment of engineering materials by means of local approaches. Mat Sci Eng R 2014;75:1–48.

[11] Smith E. Fracture initiation at the root of a blunt flaw: description in terms of Kr–Lr failure assessment curves. Int J Pres Ves Pip 1999;76:799–800.

[12] Smith E. Fracture initiation at the root of a sharp groove: description in terms of Kr–Lr failure assessment curves. Int J Eng Sci 2001;39:355–60.

[13] Matvienko YG. Local fracture criterion to describe failure assessment diagrams for a body with a crack/notch. Int J Fracture 2003;124:107–12.

[14] Matvienko YG. Development of models and criteria of notch fracture mechanics. Struct Integr

Life 2011;11:3–7.

[15] Cicero S, Madrazo V, Carrascal IA, Cicero R. Assessment of notched structural components using failure assessment diagrams and the theory of critical distances. Eng Fract Mech 2011;78:2809–25.

[16] Madrazo V, Cicero S, García T. Assessment of notched structural steel components using failure assessment diagrams and the theory of critical distances. Eng Fail Anal 2014;36:104–20.

[17] Horn AJ, Sherry AH. An engineering assessment methodology for non-sharp defects in steel structures–Part I: Procedure development. Int J Pres Ves Pip 2012;89:137–50.

[18] Horn AJ, Sherry AH. An engineering assessment methodology for non-sharp defects in steel structures–Part II: Procedure validation and constraint analysis. Int J Pres Ves Pip 2012;89:151–61.

[19] Dugdale DS. Yielding of steel sheets containing slits. J Mech Phys Solids 1960;8:100–4.

[20] Barenblatt GI. The mathematical theory of equilibrium cracks in brittle fracture. Adv Appl Mech 1962;7:55–129.

[21] Novozhilov VV. On a necessary and sufficient criterion for brittle strength. J Appl Math Mech 1969;33:201–10.

[22] Sih GC. Strain-energy-density factor applied to mixed mode crack problems. Int J Fract 1974; 10:305-21.

[23] Berto F, Lazzarin P. A review of the volume-based strain energy density approach applied to V-noches and welded structures. Theor App Fract Mech 2009; 52:183-94.

[24] Berto F, Lazzarin P. Recent developments in brittle and quasi-brittle failure assessment of engineering materials by means of local approaches. Mater Sci Eng R: Rep 2014;75:1-48.

[25] Fuentes JD, Cicero S, Berto F, Torabi AR, Madrazo V, Azizi P. Estimation of Fracture Loads in AL7075-T651 Notched Specimens Using the Equivalent Material Concept Combined with the Strain Energy Density Criterion and with the Theory of Critical Distances. Metals 2018;8:87.

[26] Torabi AR, Berto F, Razavi S.M.J. Ductile failure prediction of thin notched aluminum plates subjected to combined tension-shear loading. Theor App Fract Mech 2018;97:280-8

[27] Dowling AR, Townley CHA. The effect of defects on structural failure: a two-criteria approach. Int J Pres Ves Pip 1975;3:77–107.

[28] Harrison RP, Loosemore K, Milne I, Dowling AR. Assessment of the integrity of structures containing defects. CEGB Rep. R/H/R6, Central Electricity Generating Board; 1976.

[29] Burdekin FM, Stone DEW. The crack opening displacement approach to fracture mechanics in yielding materials. J Strain Anal Eng 1966;1:145–53.

[30] Fuentes JD, Cicero S, Ibáñez-Gutiérrez FT, Procopio I. On the use of British standard 7910 option 1 failure assessment diagram to non-metallic materials. Fatigue Fract Eng Mater Struct 2018;41:146–58.

[31] González P, Cicero S, Arroyo B, Álvarez JA. A Theory of Critical Distances based methodology for the analysis of environmentally assisted cracking in steels. Eng Fract Mech 2019;214:134–48.

[32] Neuber H. Theory of notch stresses: principles for exact calculation of strength with reference to structural form and material. Berlin: Springer Verlag; 1958.

[33] Peterson RE. Notch sensitivity. In: Sines G, Waisman JL editors. Metal fatigue. New York: McGraw Hill; 1959, p. 293–306.

[34] Creager M, Paris PC. Elastic field equations for blunt cracks with reference to stress corrosion cracking. Int J Fract Mech 1967;3:247–52.

[35] Miller AG. Review of limit loads of structures containing defects. Int J Pres Ves Pip 1988;32:197–327.

[36] Horn AJ, Budden PJ. A comparison of notch failure assessment diagram methods for assessing the fracture resistance of structures containing non-sharp defects. American Society of Mechanical Engineers, Pressure Vessels and Piping Division (Publication) 2014;6B:109176

[37] Horn AJ, Cicero S, Bannister A, Budden PJ. Validation of the Proposed R6 method for assessing non-sharp defects. American Society of Mechanical Engineers, Pressure Vessels and Piping Division (Publication) 2017;6B:131595.

[38] Cicero S, Gutiérrez-Solana F, Álvarez JA. Structural integrity assessment of components subjected to low constraint conditions. Eng Fract Mech 2008;75:3038-59.

[39] EN 573-1:2005, Aluminium and aluminium alloys - Chemical composition and form of wrought products. Brussels: European Committee for Standardization; 2005.

[40] EN 1401:2009, Plastics piping systems for water supply and for buried and above-ground drainage and sewerage under pressure - Unplasticized poly(vinyl chloride) (PVC-U). Brussels: European Committee for Standardization; 2009.

[41] ASTM E8/E8M-16ae1, Standard Test Methods for Tension Testing of Metallic Materials. West Conshohocken, PA: ASTM International; 2016.

[42] ASTM D638-14, Standard Test Method for Tensile Properties of Plastics. West Conshohocken, PA: ASTM International; 2014.

[43] ASTM E1820-20, Standard Test Method for Measurement of Fracture Toughness. West Conshohocken, PA: ASTM International; 2020.

[44] ASTM D5045-14, Standard Test Methods for Plane-Strain Fracture Toughness and Strain Energy Release Rate of Plastic Materials. West Conshohocken, PA: ASTM International; 2014.

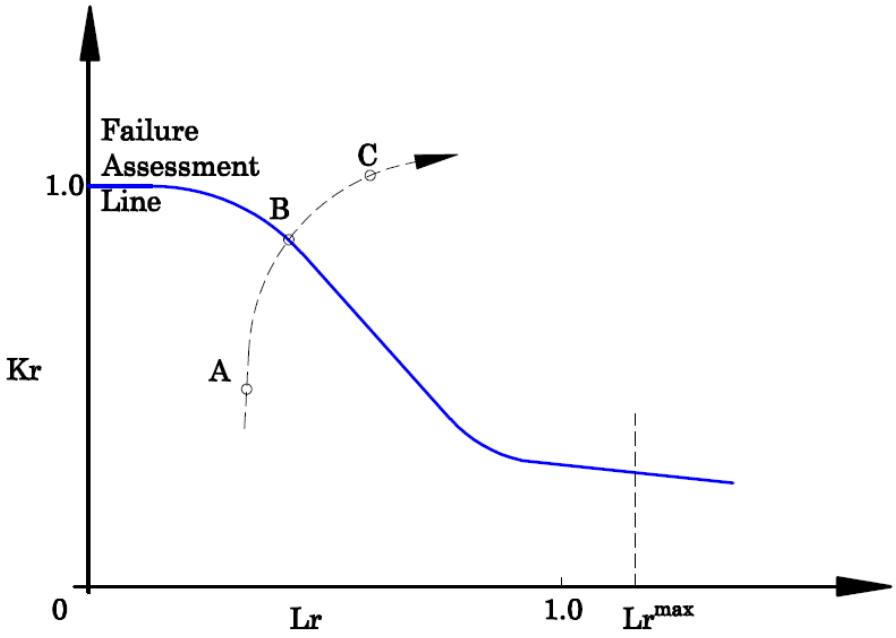

Figure 1. Schematic of the FAD methodology, showing the three possible situations: A, safe conditions; B, critical condition; C, unsafe conditions.

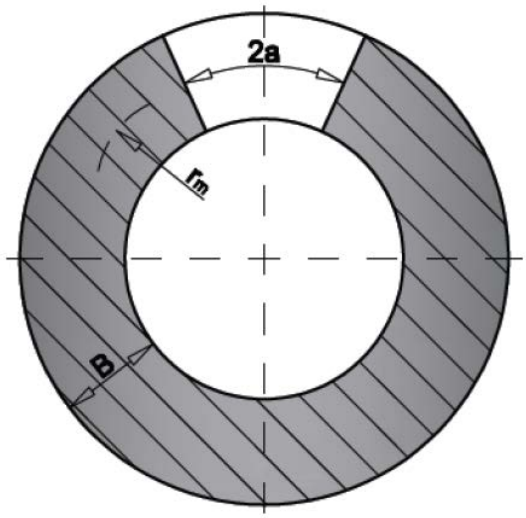

Figure 2. Geometry of the defects (through thickness notches) being analysed. 2a is the defect length, r_m is the mean radius, and B is the thickness of the tubular section.

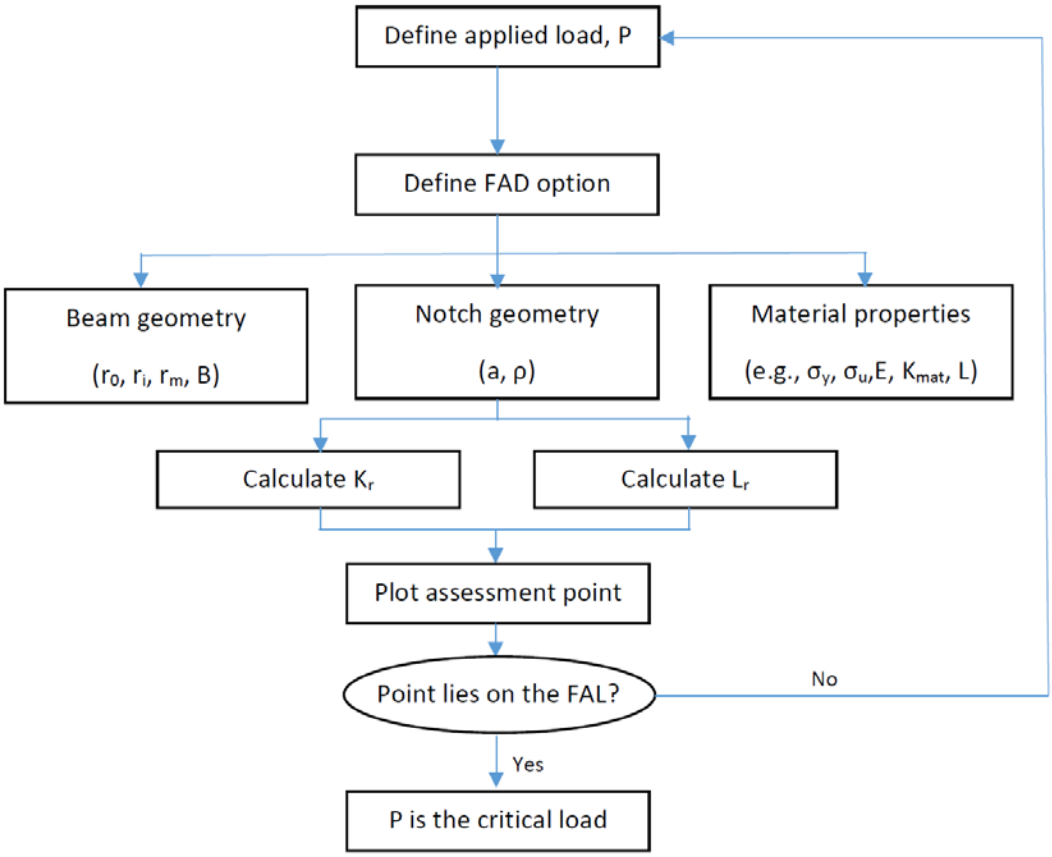

Figure 3. Flowchart of the proposed methodology.

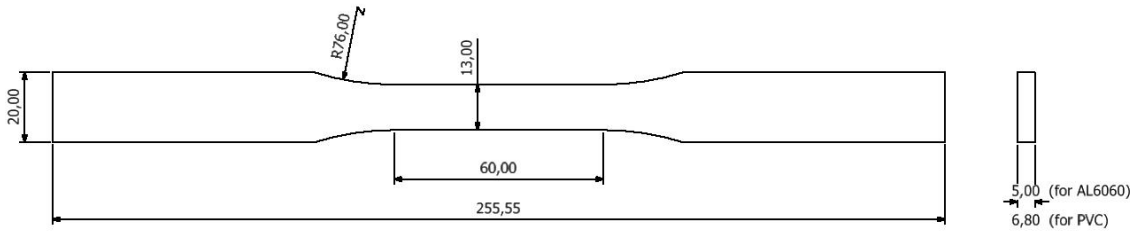

Figure 4. Tensile test specimens. Dimensions in millimetres.

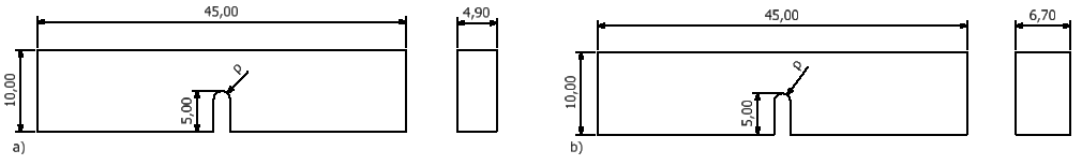

Figure 5. Schematic of fracture SE(B) specimens: a) Al6060-T66; b) PVC. Notch radius takes values of 0 mm (crack-like defects), 1 mm and 2 mm. Dimensions in mm.

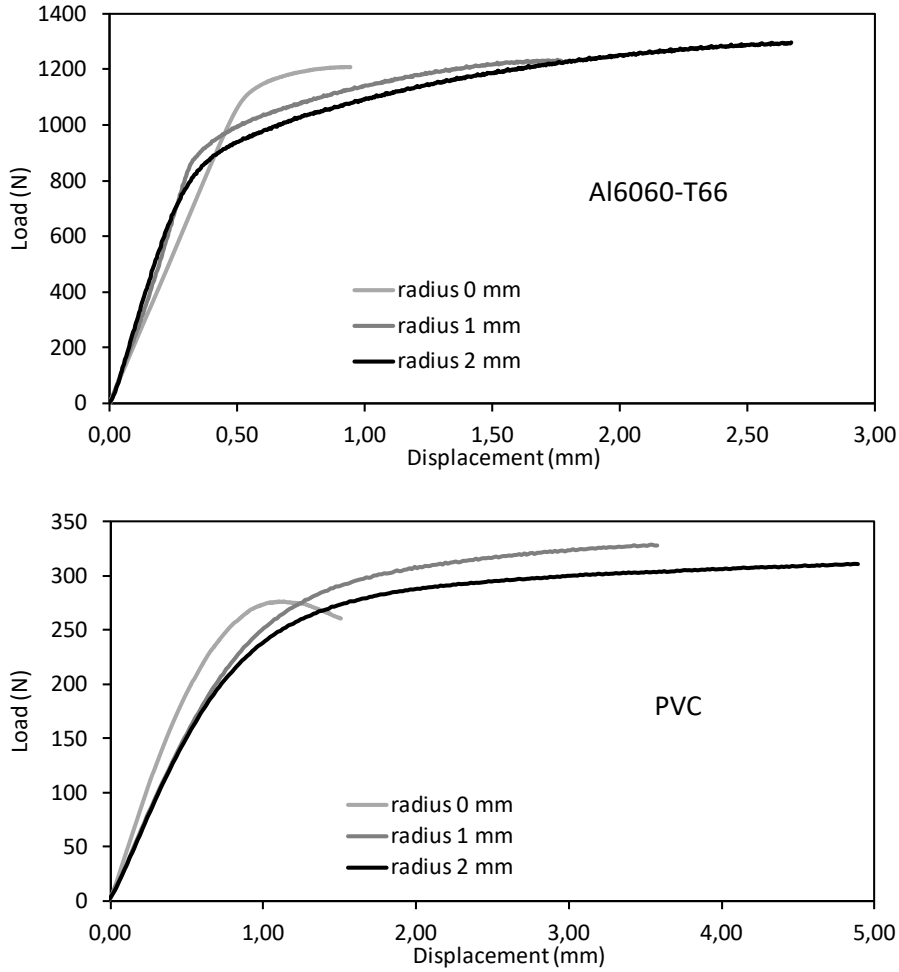

Figure 6. Load-displacement curves of some of the fracture tests. a) Al6060-T66; b) PVC

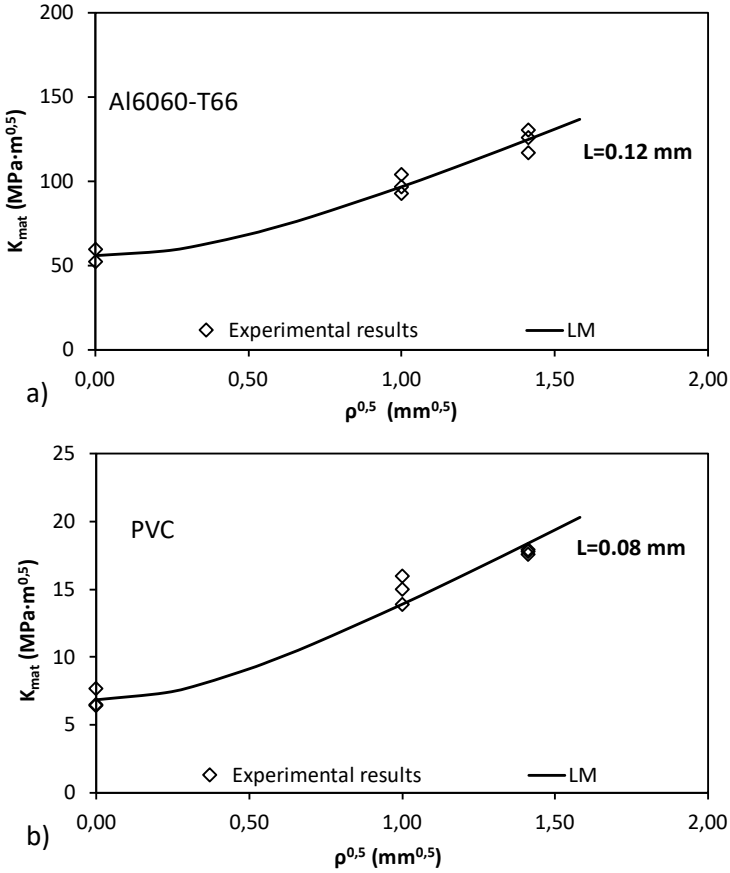

Figure 7. Fracture resistance results and estimation of L by fitting the LM equation and the least squares methodology. a) Al6060-T66; b) PVC.

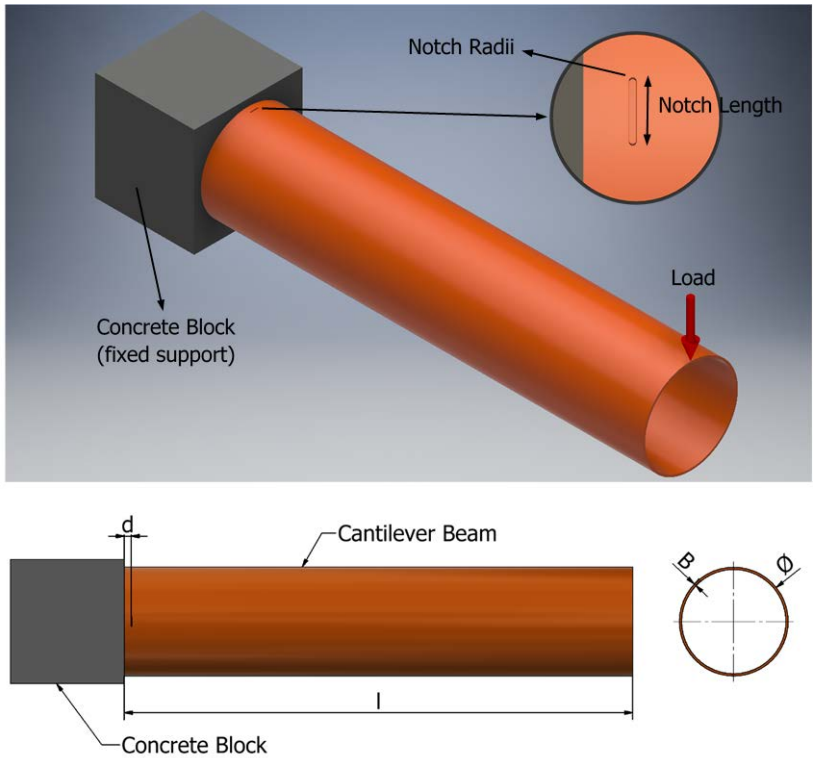

Figure 8. Schematic of tubular cantilever beams including U-notches employed. Ø refers to the outer diameter.

Figure 9. Experimental setup. Al6060-T66 (left); PVC (right).

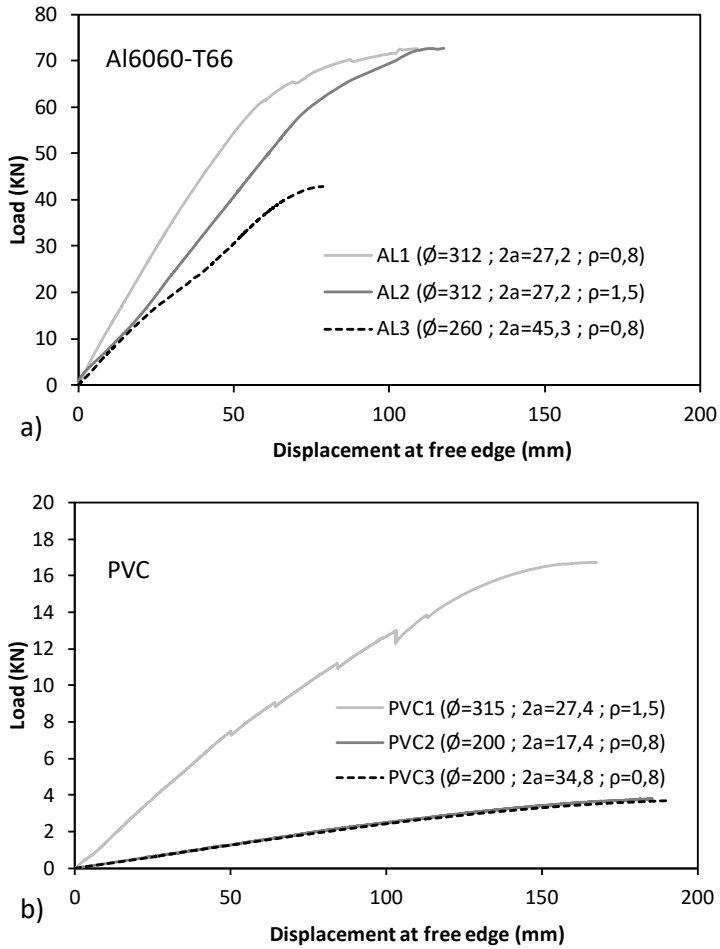

Figure 10. Load-displacement curves of the different tubular beams. a) Al6060-T66; b) PVC. Tube and defect dimensions in mm.

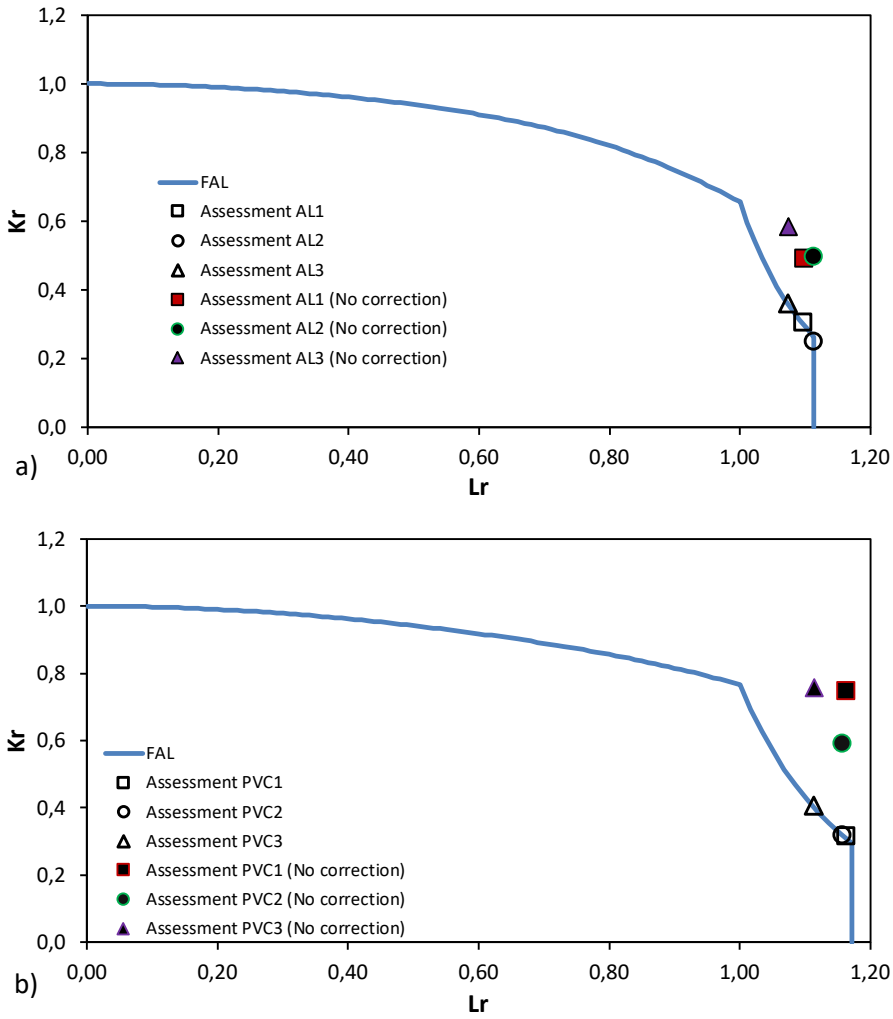

Figure 11. FAD assessments with and without notch correction. a) Al6060-T66; b) PVC.

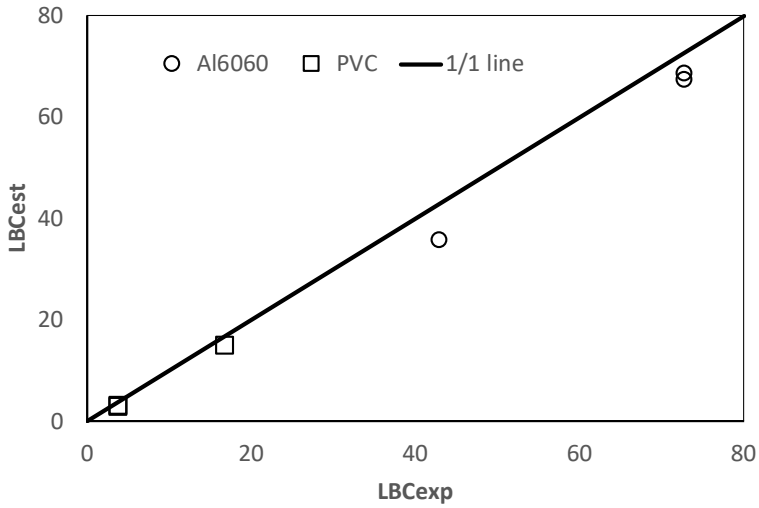

Figure 12. Comparison between the experimental results (LBC_{exp}) and the resulting estimations (LBC_{est}).

***Table 1**. Chemical composition of the 6060-T66 aluminum alloy [33] (wt.%).*

Si	Fe	Cu	Mn	Mg	Cr	Zn	Ti	Al
0,30-0,60	0,10-0,30	≤0,10	≤0,10	0,35-0,60	≤0,05	≤0,15	≤0,10	balance

Table 2. *Mechanical properties (mean and standard deviation): E, modulus of elasticity; $\sigma_{0,2}$, proof strength; σ_u, ultimate tensile strength; ε_u, elongation under maximum load.*

Material	**E (MPa)**		**$\sigma_{0.2}$ (MPa)**		**σ_u (MPa)**		**ε_u (%)**	
	Mean	**SD**	**Mean**	**SD**	**Mean**	**SD**	**Mean**	**SD**
AL 6060	70750	554	215	1.7	264	1.8	11.6	0.31
PVC	3471	199	38.6	1.5	51.1	1.1	41.1	10.9

Table 3. *Experimental results obtained in PVC and Al6060 SE(B) specimens. K^{N}_{mat} in cracked specimens corresponding to the material fracture toughness K_{mat}.*

Material	Specimen	ρ (mm)	Max. Load (N)	K^{N}_{mat} (MPa·m$^{1/2}$)
AL 6060	0-1	0	1208.8	51.8
	0-2		1341.5	59.4
	1-1	1	1235.8	96.5
	1-2		1236.2	92.6
	1-3		1226.7	103.5
	2-1	2	1296.1	125.4
	2-2		1259.2	116.4
	2-3		1259.2	130.0
PVC	0-1	0	238.0	6.41
	0-2		276.3	6.46
	0-3		290.1	7.64
	1-1	1	325.0	13.8
	1-2		328.6	14.9
	1-3		343.0	15.9
	2-1	2	311.4	17.7
	2-2		318.0	17.5
	2-3		324.7	17.8

Table 4. *Geometrical parameters of tubes and notches (see figures 2 and 5). Dimensions in mm, Load Bearing Capacity (LBC) in kN.*

Tube	Material	Ø	B	d	l	2a	ρ	LBC_{exp}	LBC_{est}
AL1	AL 6060	312.0	6.0	30.4	1451	27.2	0.8	72.65	67.50
AL2	AL 6060	312.0	6.0	27.0	1448	27.2	1.5	72.75	68.60
AL3	AL 6060	260.0	5.0	21.4	1452	45.3	0.8	42.86	35.70
PVC1	PVC	315.0	6.8	28.0	1415	27.4	1.5	16.72	14.90
PVC2	PVC	200.0	3.7	19.4	1466	17.4	0.8	3.80	3.16
PVC3	PVC	200.0	3.7	24.4	1462	34.8	0.8	3.70	2.85